16th World Conference on Earthquake, 16WCEE 2017
Santiago Chile, January 9th to 13th 2017
Paper N° 0754
Registration Code: S-T1466027652

FLOOR-TO-WALL CONNECTION BEHAVIOR IN LEDGER-FRAMED COLD-FORMED STEEL CONSTRUCTION

D. Ayhan[(1)], B.W. Schafer[(2)]

[(1)] *PhD, Postdoctoral Fellow, Johns Hopkins University, MD, USA, denizayhann@gmail.com*
[(2)] *PhD, PE, Professor, Johns Hopkins University, MD, USA, schafer@jhu.edu*

Abstract

The objective of this paper is to investigate the moment-rotation behavior of floor-to-wall connections used in ledger-framed cold-formed steel construction with full-scale experiments. Recently completed research employing full-scale shake table tests on a two-story ledger-framed cold-formed steel framed building exhibited beneficial lateral system response that far exceeded predictions. One hypothesis is that the stiffness of the floor-to-wall connections, and the repetitive nature of this connection, provided beneficial semi-rigid frame response that augmented the designed shear walls. Monotonic and cyclic full-scale connections were tested and reported here to examine the strength and stiffness, so that this hypothesis may be explored further. The test matrix is designed to evaluate the presence of floor sheathing, applied moment/shear ratio of the joist, joist-to-ledger clip angle location (inside or outside of the joist section), presence of top and bottom screws connecting the joist and ledger flanges, and location of the joist relative to the studs. The results indicate that the connection details and loading conditions drive not only the capacity but also the observed limit states. Current design for this connection assumes pure shear and is controlled by screw shear capacity. However, screw pull-out, ledger flange buckling, and stud web crippling are all observed in the testing. These findings will be used to support future 3D seismic building analysis and design and to develop improved design guidance for ledger framing.

Keywords: cold-formed steel, ledger framing, floor-to-wall connections, moment-rotation behavior, limit states.

1. Introduction

In cold-formed steel construction, three framing systems are traditionally used: ledger framing, platform framing, and balloon framing. In ledger framing, floor and roof joists are connected to the interior flange of the load-bearing studs via a combination of a ledger and clip angle. Studs terminate at the top of each floor level and are capped with a top track. Walls of the story above are stacked on a bottom track, and placed on the floor sheathing of the wall underneath. The ledger transfers floor joist loads to the vertical stud framing, and therefore, the joists are not required to be aligned with the load bearing studs, as shown in Fig. 1.

Fig 1 – Ledger framing connection examples

The seismic behavior of light-framed cold-formed steel (CFS) buildings was recently investigated with experimental characterization in different scales: fastener, member and full-scale in the CFS-NEES project [1]. The CFS-NEES building has used ledger framing for floor-to-wall connections as shown in Fig. 2. In full scale tests, it was observed that the CFS-NEES building performance exceeded design expectations. The contribution of other structural and even non-structural members; such as floor-to-wall connections, to the lateral load resisting system should be considered along with the shear walls that are designed for lateral seismic demands.

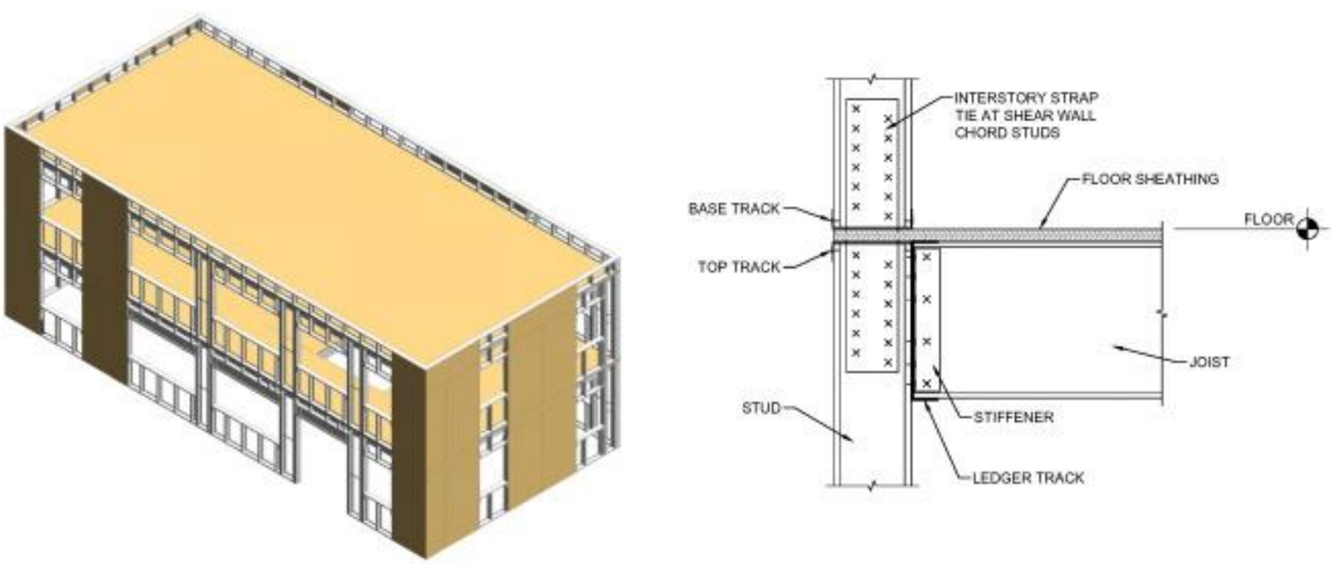

(a) (b)

Fig 2 – CFS-NEES archetype building utilized to organize research and for full-scale testing [1] (a) Rendering from BIM model, only shear walls and diaphragm sheathed, (b) detail at shear wall chord

The framing action between the floor joists and wall studs is related to the stiffness of the floor-to-wall connections. Discontinuity of the load path at the connection point, and stiffness of the thin-walled members, makes rigid or full moment resisting connections difficult to achieve in practical construction. Therefore, semi rigid behavior is typical and quantifying the stiffness, or more generally the moment-rotation response of existing connections, is sought through sub-assemblage experiments on floor-to-wall connections.

Current code guidance for the joist-to-ledger connection assumes pure shear and focuses primarily on insuring the adequacy of the clip angle screws in shear. This is inadequate for understanding the actual connection behavior; accordingly, full-scale floor-to-wall connections are tested to explore their behavior. The testing program is designed to evaluate i) the presence of floor sheathing, ii) the presence of top and bottom screws connecting the joist and ledger flanges, iii) the applied loading location and iv) the clip angle location, all depending on the joist location relative to the wall studs: i.e. (a) mid studs, (b) close, or (c) on stud. The effect of these parameters on response under monotonic loading has previously been reported by the authors [2-4]. The purpose of this paper is to provide test results conducted under cyclic loading and compare with the monotonic tests in an examination of the floor-to-wall connection behavior. This work is a part of a broader study on ledger-framing construction to support future 3D seismic building analysis and design for cold-formed steel framing.

2. Experimental program

The experimental program was created to investigate floor joist-to-wall connection behavior in a ledger-framed CFS building. Specimen cross-sections were selected according to the CFS-NEES building [1], which had a floor diaphragm framed with 1200S250-97 joists and 1200T200-97 rim tracks (ledgers) sheathed with 7/16 in. (1.11 cm) thick OSB sheathing and first story gravity walls framed with two 600S162-54 studs and two 600T150-54 tracks. A clip angle of 1.5x1.5-54 was used to attach joists to ledgers. The cross-section properties are defined in AISI S200 [5].

2.1 Test matrix

The parameters to be evaluated in the test program were 1. presence of floor sheathing, 2. presence of top and bottom screws connecting joist and ledger flanges, 3. loading location (applied moment/shear ratio), and 4. clip angle location (inside or outside of joist section), all depending on floor joist locations relative to studs: mid studs, near stud, and on stud. Accordingly, specimens are grouped in four test series. The test matrix is presented in Table 1. The first series was used to examine the effect of floor sheathing for three different joist locations. The specimens of the first series were constructed with top and bottom screws connecting the ledger and joist flanges, a clip angle attached to the inside of joist section, and load was applied at a distance of 5 in. (12.7 cm) from the connected end (to cause the maximum shear force). From the first series, the specimens having floor sheathing are denoted as “reference specimens” hereafter and used to investigate secondary parameters with the specimens of the second, third and fourth series.

All configurations were built twice and tested under both monotonic and cyclic loadings. In total 30 experiments were conducted. The results of the monotonic testing have been previously reported [2-4].

Table 1 – Test Matrix

		principal parameters		secondary parameters		
	test no	joist location	floor sheathing	top & bottom screws	clip angle location	loading location
first series	1	mid studs		✓	inside	connected end *(5 in. away from connection)*
	2	near stud		✓		
	3	on stud		✓		
	4	mid studs	✓	✓		
	5	near stud	✓	✓		
	6	on stud	✓	✓		
second series	13	mid studs	✓		inside	connected end
	14	near stud	✓			
	15	on stud	✓			
third series	19	mid studs	✓	✓	inside	free end *(50 in. away from connection)*
	20	near stud	✓	✓		
	21	on stud	✓	✓		
fourth series	25	mid studs	✓	✓	outside	connected end
	26	near stud	✓	✓		
	27	on stud	✓	✓		

Note: The total test matrix consists of 30 tests. The missing numbers are for the cyclic tests of the same configurations.

2.2 Test setup and instrumentation

Typical specimen details are depicted in Fig. 3 and 4. The generic joist-to-wall connection specimen consists of a stud frame, a ledger beam, a joist, a clip angle, and floor sheathing. The stud frame includes two 32 in. (81.3 cm) long studs attached to the 24 in. (61.0 cm) long top and bottom tracks by four No. 10 screws. A 24 in (61.0 cm) ledger track is connected to one side of the studs via six No. 10 screws through the ledger web and the stud flange. A 62 in (157.5 cm) joist is connected to the web of the ledger via a clip angle connected by four No. 10 screws per leg. Where desired, both top and bottom flanges of the joist are connected to the ledger using a single No. 10 screw and OSB sheathing is attached to the top of the track and joist and connected by No. 10 screws. A track is attached to the end of the joist to enable lateral support (by 3/4 in. (1.9 cm) threaded rods) to restrain the lateral deformation and restrict twist.

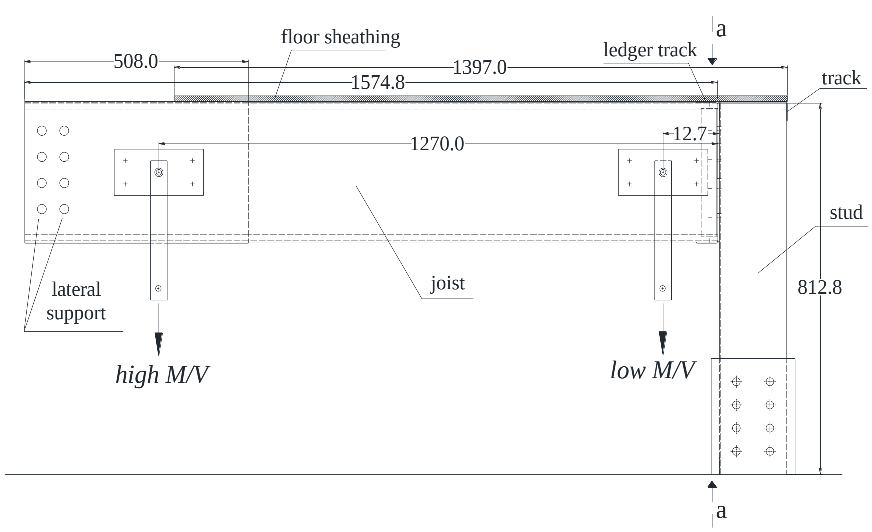

Fig. 3 – Specimen details with a side view including two loading locations (dimensions in mm)

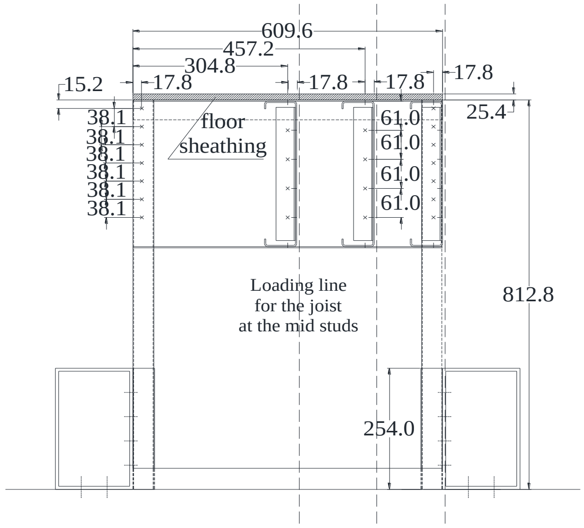

Fig. 4 – a-a section from Fig 3. including three joist locations (dimensions in mm)

A vertical load was applied to the joist by a hydraulic actuator at a distance of either 5 in. (12.7 cm), the closest possible point to the connection to cause the maximum shear force or 50 in. (127.0 cm) away from the connected location to cause maximum moment. The sketch of the test setup is illustrated in Fig. 5. A cyclic displacement history was applied at the loading point using a customized control program receiving feedback with a displacement rate based on a stain rate of 0.05 m/m/sec. The displacement rate for monotonic tests was derived based on a constant strain rate of 0.005 m/m/sec.

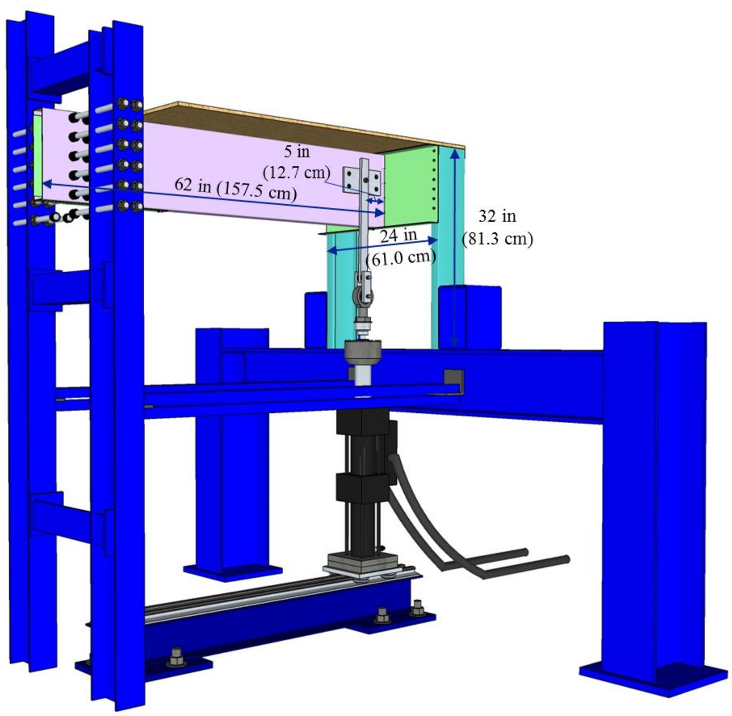

Fig. 5 – Joist-to-wall connection test setup sketch (blue is testing rig)

The instrumentation consists of 12 position transducers (PTs) to measure the necessary deformations to calculate the absolute rotations of connection ($\theta_{con} = \theta_J - \theta_S$), joist ($\theta_J$), stud frame ($\theta_S$) and ledger track ($\theta_L$), and the relative rotations of the joist to the ledger track (θ_{JL}) and clip angle leg (θ_{JA}), as shown in Fig. 6. The stud frame rotation (θ_S) is calculated with linear interpolation from the stud rotations (θ_{S1} for stud away from joist and θ_{S2} stud close to joist) depending on joist location.

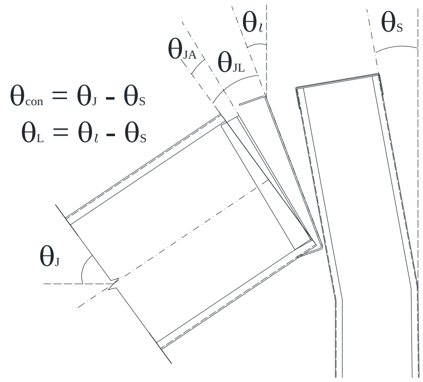

Fig. 6 – Rotation components of the connection

2.3 Displacement controlled testing protocol

The displacement-controlled testing protocol (see Fig. 7) is adapted from the FEMA 461 quasi-static cyclic deformation-controlled testing protocol. The FEMA 461 protocol was developed originally for testing of drift sensitive nonstructural components, but is applicable also to drift sensitive structural components. FEMA 461 uses a targeted maximum deformation amplitude, Δ_m, and a targeted smallest deformation amplitude, Δ_0, as reference values, and a predetermined number of increments (steps), n, to determine the loading history (a value of n ≥ 10 is recommended). The amplitude a_i of the step-wise increasing deformation cycles is given by the equation $a_{i+1}/a_n = 1.4\ (a_i/a_n)$, where a_1 is equal to Δ_0 (or a value close to it) and a_n is equal to Δ_m (or a value close to it). Two cycles are to be executed for each amplitude. If the last damage state has not yet occurred at the target value Δ_m, the loading history is continued by using further increments of amplitude of $0.3\Delta_m$ to obtain fragility data and hysteretic response characteristics of building components for which damage is best predicted by imposed deformations.

The protocol is adapted here for a one-sided application, see Fig. 7. The protocol is anchored to the elastic displacement according to what is observed in monotonic tests at the fourth step (i.e., seventh and eight cycles). The number of steps (n) is chosen as 13 to be applied on all of the tests as provided in Table 2. An extra step has been added at the end of 13th step with an increment of $0.3\Delta_m$. Thus, 26 cycles are completed in cyclic load, and 27th and 28th cycles are run only if the most severe damage has not yet occurred.

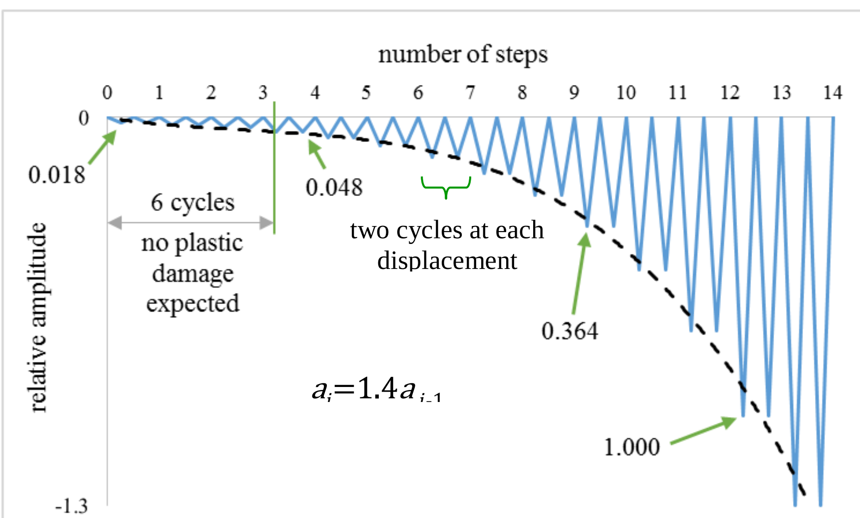

Fig. 7 – Sketch of deformation controlled FEMA 461 testing protocol

Table 2 – Relative loading history deformation amplitudes

n	1	2	3	4	5	6	7	8	9	10	11	12	13	14
a_i/Δ_m	*0.018*	*0.025*	*0.035*	*0.048*	*0.068*	*0.095*	*0.133*	*0.186*	*0.260*	*0.364*	*0.510*	*0.714*	*1.000*	*1.300*

3. Experimental Results

Moment-rotation (M-θ) response was obtained for all joist-to-wall connection tests. Experimental values for connection rotations were considered as the absolute joist rotation by excluding stud frame rotation (Fig. 6). Experimental values of the moment are calculated as M=*d*V, where V is the measured vertical load at the actuator and *d* is the distance of the loading location to the connection (50 in. [127.0 cm] for the tests of third series, 5 in [12.7 cm] for all others).

3.1 Limit states

The displacement protocol was continued to the maximum stroke of the hydraulic actuator (6 in., 152.4 mm) or until test setup limits for the joist end to move were reached. Three primary limit states are observed: pull-out of fasteners connecting the ledger to the stud, buckling of the ledger bottom flange, and stud web crippling (Fig. 8). Following the primary limit states ledger section deformation, fastener tilting and/or floor sheathing bending are also observed as secondary limit states. These limit states are newly observed in this experimental study.

a) fastener pull-out b) ledger bottom flange buckling c) stud web crippling

Fig. 8 – Primary limit states observed in the tests

The primary and secondary limit states observed in the monotonic and cyclic tests are tabulated in Table 3. The primary limit states driving the failure remain the same under monotonic and cyclic loading. All of the specimens having the joist located mid-distance between the studs failed due to ledger bottom flange buckling. Stud web crippling was the primary limit state observed for specimens having the joist ¼ of the distance between studs or aligned with the studs, except specimens T2 and T8 without floor sheathing, and specimens T20 and T23 which had the highest moment/shear ratio. The absence of floor sheathing caused T2 and T8 to fail because of fastener pull-out, and T20 and T23 failed due to ledger bottom flange buckling rather than stud web crippling. All specimens with the joists aligned with the stud were exhibited stud web crippling as the primary limit state.

Table 3 – Limit states observed in the monotonic and cyclic tests

		test no	Ledger flange buckling	Stud web crippling	Fastener pull-out	Ledger section deformation	Fastener tilting	Floor sheathing bending
first series	Monotonic (M)	T1- mid studs (no sheathing)	P					
		T2- near stud (no sheathing)			P			
		T3- on stud (no sheathing)		S	P			
		T4- mid studs (reference)	P				S	S
		T5- near stud (reference)		P		S	S	
		T6- on stud (reference)		P	S		S	
	Cyclic (C)	T7- mid studs (no sheathing)	P			S		
		T8- near stud (no sheathing)			P	S		
		T9- on stud (no sheathing)		P	S			
		T10- mid studs (reference)	P				S	S
		T11- near stud (reference)		P		S	S	
		T12- on stud (reference)		P			S	
second series	M	T13- mid studs (no screws)	P					S
		T14- near stud (no screws)		P				
		T15- on stud (no screws)		P	S			
	C	T16- mid studs (no screws)	P				S	
		T17- near stud (no screws)		P		S		
		T18- on stud (no screws)		P			S	S
third series	M	T19- mid studs (high M/V)	P				S	
		T20- near stud (high M/V)	P				S	
		T21- on stud (high M/V)		P	S		S	
	C	T22- mid studs (high M/V)	P					S
		T23- near stud (high M/V)	P				S	S
		T24- on stud (high M/V)		P	S		S	S
fourth series	M	T25- mid studs (clip angle)	P				S	S
		T26- near stud (clip angle)		P		S	S	
		T27- on stud (clip angle)		P			S	
	C	T28- mid studs (clip angle)	P					S
		T29- near stud (clip angle)		P		S	S	
		T30- on stud (clip angle)		P			S	

P: primary limit state, S: secondary limit state, M: monotonic, C: cyclic

3.2 Moment-rotation capacities

Table 4 summarizes the maximum applied shear force (V_{max}) and moment (M_{max}), joist-to-ledger connection rotation (θ_{con}) corresponding to M_{max}, and the stiffness (k_1 and k_2) observed prior to M_{max}. The pre-peak stiffness is characterized as bilinear and represented by k_1 and k_2 as shown in Fig. 9. The absolute ledger rotation (θ_L), rotations between joist and ledger (θ_{JL}), between joist and angle (θ_{JA}), and stud frame rotation (θ_S) corresponding to M_{max} are also provided. The maximum actuator force (V_{max}) was measured in T16, the cyclic test of the sheathed specimen having joist on mid studs with no bottom and top screws connecting the joist and ledger flanges. The maximum measured V_{max} is well below the clip angle screw shear capacity which is 25.35kN for four No.10 screws. The maximum moment (M_{max}) was observed in monotonic test T21, this sheathed specimen had the joist aligned with the stud and the high applied moment/shear ratio.

The maximum connection rotation is measured in the non-sheathed specimen, T7, with the joist at mid-distance between the studs under cyclic loading. The maximum initial stiffness of the connection is measured in T20, a monotonic test of a specimen having the joist ¼ of the distance between studs under high moment/shear ratio. For comparison, the measured maximum stiffness is only 2% of the fixed connection stiffness (5400kNm). It is worth noting that all specimens were able to provide a connection rotation ranging between 0.021 and 0.135 radian prior to failure.

Table 4 – Measured quantities for floor-to-wall connection tests

		test no	V_{max} (kN)	M_{max} (kNm)	θ_{con} (rad)	k_1 (kNm)	k_2 (kNm)	θ_L (rad)	θ_{JL} (rad)	θ_{JA} (rad)	θ_S (rad)
first series	Monotonic (M)	T1- mid studs (no sheathing)	10.42	1.42	0.045	47.233	26.050	0.042	0.005	0.001	0.024
		T2- near stud (no sheathing)	12.67	1.61	0.040	66.298	32.318	0.036	0.003	0.001	0.033
		T3- on stud (no sheathing)	8.78	1.12	0.037	35.142	27.457	0.018	0.007	0.006	0.031
		T4- mid studs (reference)	14.98	1.90	0.033	98.612	45.112	0.028	0.001	0.001	0.033
		T5- near stud (reference)	16.80	2.13	0.035	103.422	47.163	0.032	0.002	0.000	0.037
		T6- on stud (reference)	13.11	1.67	0.049	74.774	24.701	0.035	0.007	0.007	0.038
	Cyclic (C)	T7- mid studs (no sheathing)	16.76	2.13	0.135	33.024	11.644	0.172	0.008	0.001	0.018
		T8- near stud (no sheathing)	13.85	1.76	0.069	46.786	19.632	0.048	0.003	0.001	0.041
		T9- on stud (no sheathing)	8.47	1.08	0.056	42.457	13.934	0.031	0.008	0.007	0.028
		T10- mid studs (reference)	15.56	1.98	0.043	55.790	41.003	0.024	0.003	0.001	0.034
		T11- near stud (reference)	16.14	2.05	0.059	50.442	28.604	0.036	0.002	0.000	0.032
		T12- on stud (reference)	14.01	1.78	0.051	61.343	27.184	0.029	0.004	0.003	0.022
second series	M	T13- mid studs (no screws)	12.83	1.63	0.038	51.561	38.706	0.022	0.003	0.000	0.025
		T14- near stud (no screws)	15.78	2.00	0.045	52.124	40.611	0.025	0.002	0.000	0.030
		T15- on stud (no screws)	14.43	1.83	0.054	67.897	25.537	0.027	0.006	0.006	0.016
	C	T16- mid studs (no screws)	18.61	2.36	0.117	55.196	14.247	0.101	0.008	0.003	0.027
		T17- near stud (no screws)	14.85	1.89	0.045	49.176	38.136	0.027	0.003	0.000	0.028
		T18- on stud (no screws)	14.39	1.83	0.047	51.795	33.404	0.024	0.007	0.006	0.026
third series	M	T19- mid studs (high M/V)	1.10	1.39	0.021	70.675	61.575	0.017	0.001	0.000	0.014
		T20- near stud (high M/V)	1.64	2.08	0.031	104.580	54.139	0.024	0.002	0.001	0.020
		T21- on stud (high M/V)	2.41	3.06	0.073	51.405	38.139	0.051	0.005	0.008	0.007
	C	T22- mid studs (high M/V)	1.32	1.67	0.030	59.948	55.581	0.020	0.001	0.001	0.018
		T23- near stud (high M/V)	1.57	1.99	0.031	91.186	52.633	0.020	0.002	0.001	0.019
		T24- on stud (high M/V)	2.04	2.59	0.081	55.683	24.950	0.054	0.005	0.007	0.005
fourth series	M	T25- mid studs (clip angle)	13.18	1.67	0.041	38.791	42.528	0.022	0.003	0.002	0.020
		T26- near stud (clip angle)	16.69	2.12	0.058	42.808	33.268	0.033	0.002	0.001	0.025
		T27- on stud (clip angle)	14.06	1.79	0.056	48.849	25.682	0.031	0.003	0.001	0.032
	C	T28- mid studs (clip angle)	16.26	2.07	0.050	50.487	36.403	0.027	0.003	0.001	0.032
		T29- near stud (clip angle)	16.57	2.10	0.052	57.981	34.020	0.030	0.002	0.001	0.033
		T30- on stud (clip angle)	12.73	1.62	0.059	52.581	20.669	0.027	0.003	0.001	0.038

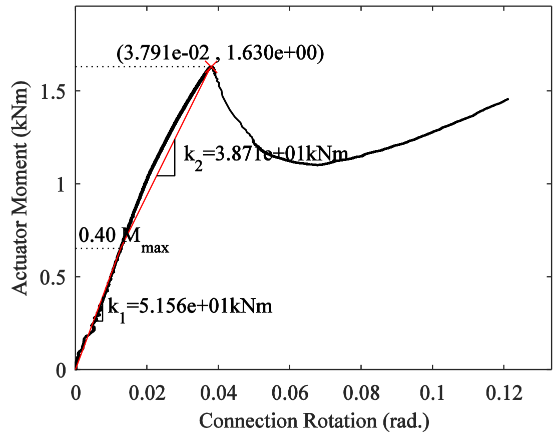

Fig. 9 – Example of stiffness degradation observed on test results (T13)

3.3 Moment-rotation response envelope comparisons

For all cyclic tests, the moment-rotation response started as linear elastic for at least the first 3 steps (six cycles). Limit states are typically observed after the 10th step (20 cycles) in a pattern similar to the monotonic members as illustrated in Fig. 10a, 11a and 12a. The specimens subjected to cyclic loading exhibited the same limit states as their monotonic counterparts; however, comparing the hysteretic response across limit states is challenging because of the different parameters considered in this study. The initial stiffness, failure moments, and strength degradations vary for different configurations.

Here, cyclic-monotonic test comparisons are provided only for the third series where the effect of applied moment/shear ratio is examined (Fig. 10b, 11b and 12b). If one compares cyclic response envelopes to the monotonic responses, similar characteristics can be observed across the different locations of joist relative to the studs. Initial stiffness does not change and the post-failure behavior has similar trends between the monotonic and cyclic response. Tests with the joist on (aligned) or near (1/4 distance) of the stud, i.e. Fig. 11 and 12 exhibit cyclic degradation in the maximum strength as the stud web crippling is engaged. The test with the joist mid-distance between the studs exhibits no cyclic degradation and in fact has a higher capacity in the cyclic tests demonstrating significant strength sensitivity in the observed ledger bottom flange buckling limit state.

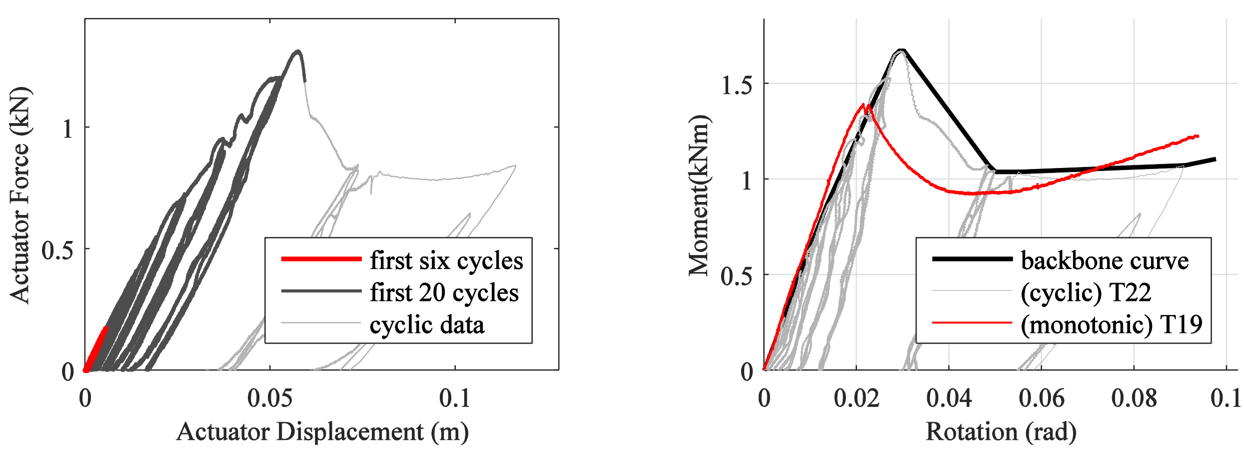

(a) (b)

Fig. 10 – Results for the specimens having joist on mid studs with high applied M/V ratio, (a) the adaptation of FEMA 461 loading protocol, (b) comparisons of monotonic and cyclic responses of the connection

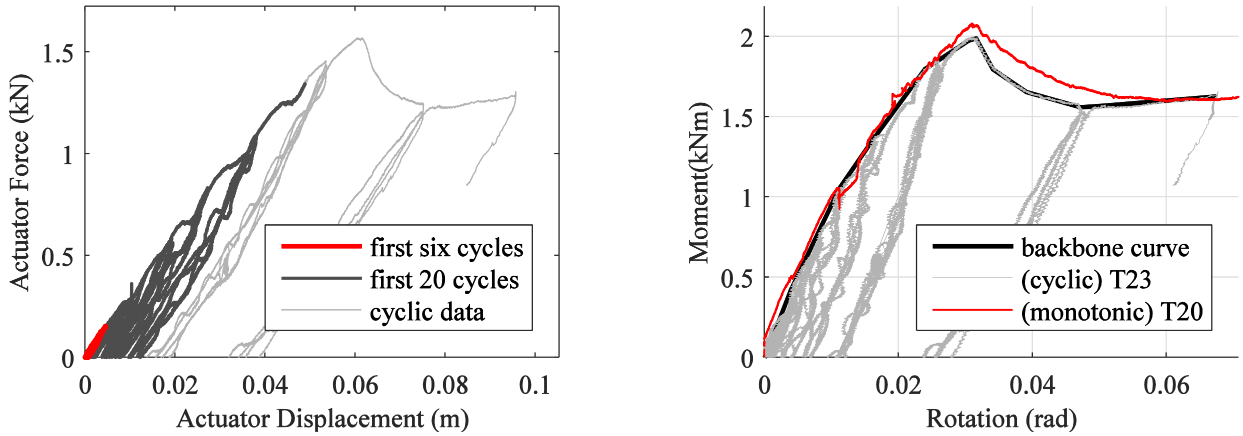

(a) (b)

Fig. 11 – Results for the specimens having joist near stud with high applied M/V ratio, (a) the adaptation of FEMA 461 loading protocol, (b) comparisons of monotonic and cyclic responses of the connection

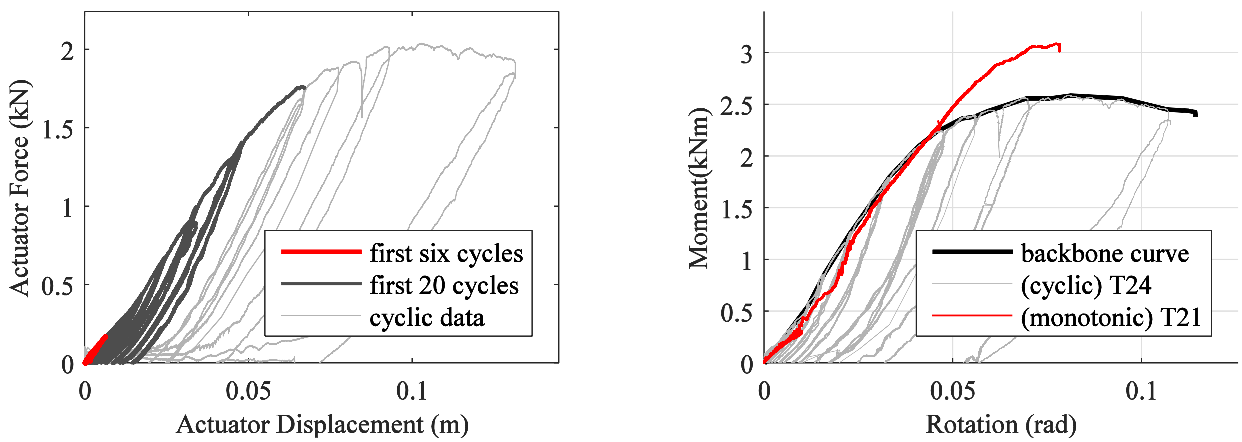

(a) (b)

Fig. 12 – Results for the specimens having joist on stud with high applied M/V ratio, (a) the adaptation of FEMA 461 loading protocol, (b) comparisons of monotonic and cyclic responses of the connection

4. Conclusions

An experimental program was conducted to investigate the floor-to-wall connection behavior in ledger-framed cold-formed steel construction. Three different joist locations: mid-distance between studs, ¼ distance between studs, and aligned on the stud, are considered across an investigation of connection parameters; including: presence of floor sheathing, applied moment/shear ratio, clip angle location (inside or outside of the joist section), and presence of top and bottom screws connecting the joist and ledger flanges. Tests were conducted under monotonic and cyclic loading for a total of 30 experiments. The primary limit states observed in the tests were fastener pull-out, ledger bottom flange buckling, and stud web crippling. These are newly observed limit states in these connections and not currently checked in design. Design typically consider screw shear in the joist-to-ledger clip angles, this limit state was not observed in the tests. Primary limit states observed in the monotonic tests remained the same in the cyclic tests: local buckling of ledger flange for connections with the joists mid-distance between the studs, and typically stud web crippling for connections where the joist is aligned or near the stud. Pull-out of the ledger to joist screws was also observed in tests without floor sheathing. The connections provided post-failure strength and stiffness even after the observed primary limit states. Cyclic strength degradation and cyclic stiffness degradation varied across the different parameters. Building modeling utilizing this information is anticipated in the future.

5. Acknowledgements

This project was partially funded by the U.S. National Science Foundation under Grant No. (NSF-CMMI #1041578). Cold-formed steel products were donated by ClarkDietrich, and fasteners from Simpson Strong-Tie. Laboratory assistance from John Boutillier and Nick Logvinovsky was much appreciated. Any opinions, findings, and conclusions or recommendations expressed in this material are those of the author(s) and do not necessarily reflect the views of the National Science Foundation, or any of the participating companies.

5. References

[1] Schafer B.W., Ayhan D., Leng J., Liu P., Padilla-Llano D., . Peterman K.D, Stehman M., Buonopane S.G., Eatherton M., Madsen R., Manley B., Moen C.D., Nakata N., Rogers C., Yu C (2016): Seismic Response and Engineering of Cold-formed Steel Framed Buildings. *Structures*, doi:10.1016/j.istruc.2016.05.009.

[2] Ayhan D, Qin Y, Torabian S, Schafer BW (2015): Characterizing joist-ledger performance for cold-formed steel light frame construction. *8th International Conference on Advances in Steel Structures*, Lisbon, Portugal, Jul. 22-24.

[3] Ayhan D, Schafer BW (2016): Stiffness, stability, and strength of floor-to-wall connections in ledger-framed cold-formed steel construction. *Annual Stability Conference Structural Stability Research Council*, Orlando, Florida, April 12-15.

[4] Ayhan D, Schafer BW (2016): The effect of M/V ratio on ledger-framing performance of cold-formed steel buildings. *The International Colloquium on Stability and Ductility of Steel Structures*, Timisoara, Romania, May 30 - June 1.

[5] AISI S200 (2012): North American Standard for Cold-Formed Steel Framing – General Provisions, American Iron and Steel Institute, Washington, DC.